Supplementary Information

Rationally integrated nickel sulfides for lithium storage: S/N co-doped carbon encapsulated NiS/Cu_2S with greatly enhanced kinetic property and structural stability

Weiliang Peng[1, 2#], Junhao Zhang[1, 2#], Shaobo Li[1, 2*], Jinxia Liang[1], Renzong Hu[1, 2], Bin Yuan[1, 2*], Guojie Chen[3*]

[1]*School of Materials Science and Engineering, South China University of Technology, Guangzhou 510640, P.R. China*

[2]*Key Laboratory of Advanced Energy Storage Materials of Guangdong Province, P.R. China*

[3]*Guangdong-Hong Kong-Macao Joint Laboratory for Intelligent Micro-Nano Optoelectronic Technology, Foshan University, 528225, P. R. China*

Email: lishb08@scut.edu.cn; apsheng@scut.edu.cn or 512088102@qq.com

[#]These authors contributed equally.

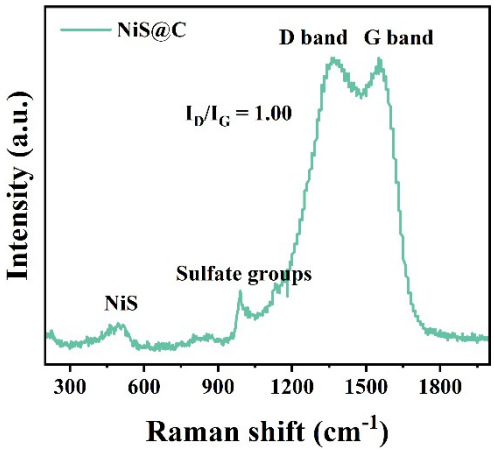

Fig. S1 The Raman spectrum of NiS@C.

The Raman spectrum of NiS@C shows similar results with NiS/Cu_2S@N/S-C. It is worth mentioning that the additional peak at 990 cm^{-1} in the Raman spectrum of NiS@C corresponds to the characteristic peak of sulfate groups[1, 2], which is ascribed to the inevitable surface sulfur oxidation of NiS@C.

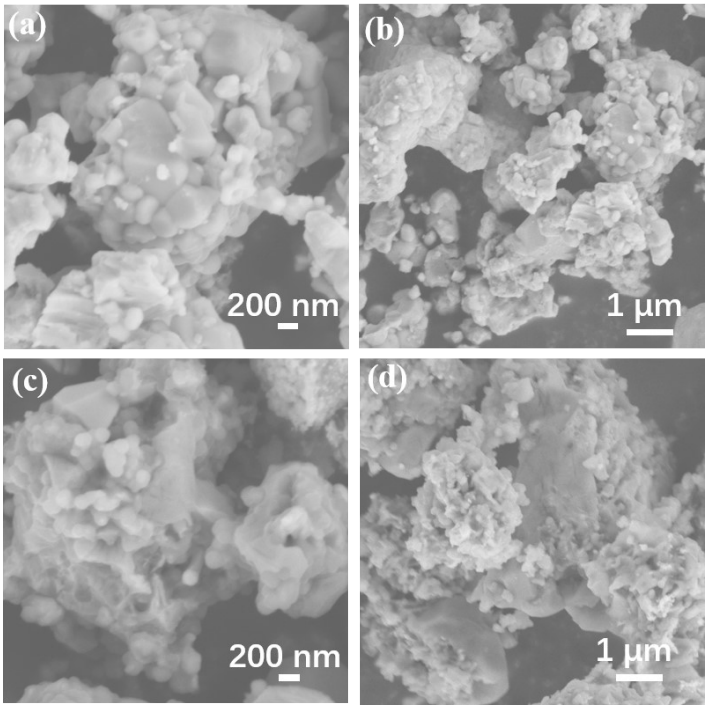

Fig. S2 SEM images of (a)-(b)Pure-NiS and (c)-(d) NiS@C.

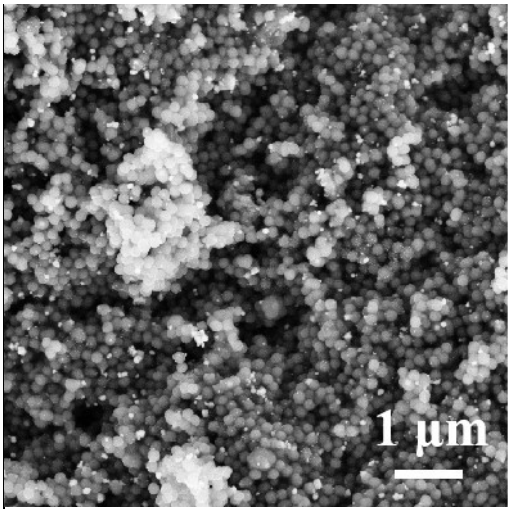

Fig. S3 SEM low magnification image of NiS/Cu_2S@N/S-C.

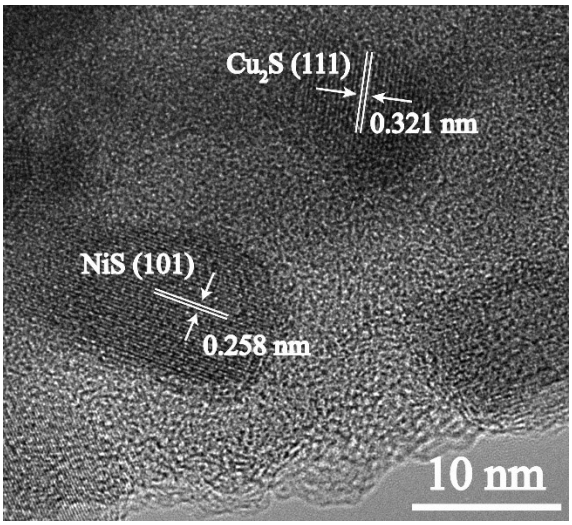

Fig. S4 HRTEM image of NiS/Cu_2S@N/S-C.

Table S1. The results of ICP-OES for the NiS/Cu_2S@N/S-C

Elements	concentration (mg/L)
Ni	9.1468
Cu	2.4830

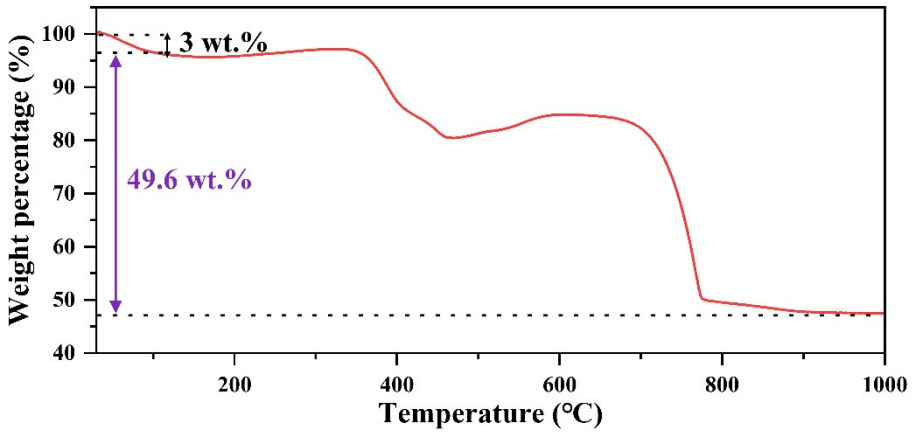

Fig. S5 TGA curve of the NiS/Cu_2S@N/S-C

Firstly, ICP-OER was performed to confirm the content of NiS and Cu_2S. According to the results of ICP-OES (Table S1), the mass ratio of Ni and Cu in the NiS/Cu_2S@N/S-C is 3.68:1, suggesting the mass ratio of NiS and Cu_2S is 4.54:1. Meanwhile, the atomic ratio of Ni and Cu can be calculated to 4:1, indicating the molar ratio of NiS and Cu_2S is 8:1. Furthermore, the TGA test was conducted to was obtained to calculate the content of carbon under air atmosphere from 30 to 1000°C with a heating rate of 10°C/min. As shown in Fig. S5, the mass loss below 100°C (3 wt.%) is ascribed to the loss of adsorption species (*e.g.* adsorption water) on the surface of the NiS/Cu_2S@N/S-C. The following heating process involved combustion of carbon and redox reaction of metal sulfides with oxygen, that is, the process from NiS/Cu_2S@N/S-C to NiO/CuO, SO_2 and combustion product of N/S-C. Accordingly, the overall mass loss (49.6 wt.%) can be equivalent to the mass of sulfur in NiS/Cu_2S and the mass of N/S-C minus the mass of oxygen in the final metal oxides. Hence, the weight percentage of NiO/CuO was calculated as 47.4 wt.% ((100 - 3 - 49.6) wt.%), further suggesting the weight percentage of NiS and Cu_2S are 45.4 and 9.9 wt.% based on the molar ratio of Ni/Cu and the difference of relative molecular mass between NiO/CuO and NiS/Cu_2S.

Furthermore, the weight percentage of N/S-C can be equivalent to 100 wt.% minus the sum of the weight percentage of adsorption species (3 wt.%) and the weight percentage of NiS/Cu_2S ((45.4 + 9.9) wt.%), that is 41.7 wt.%. Thus, the actual weight percentages of the Cu_2S, NiS and N/S-C in the NiS/Cu_2S@N/S-C hybrids can be normalized to 9.9, 45.4 and 41.7 wt.%, respectively.

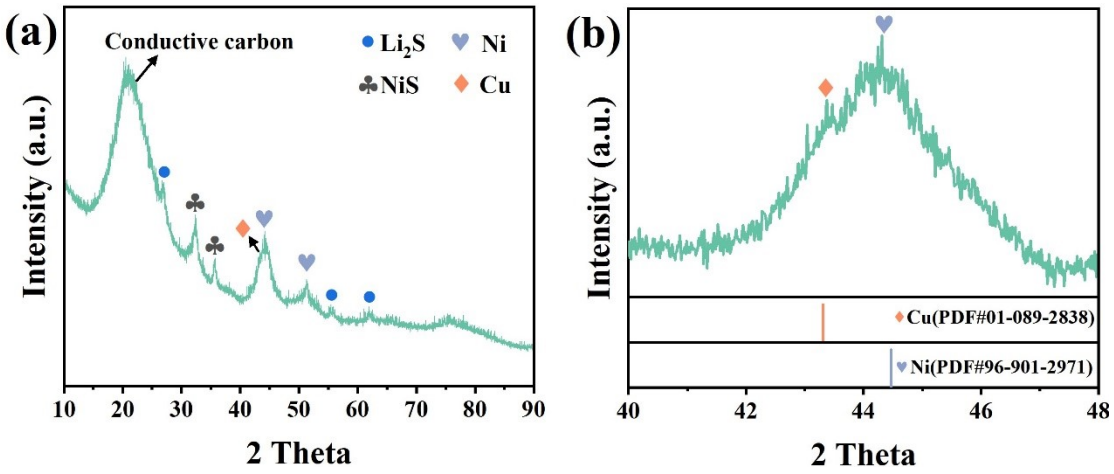

Fig. S6 (a) The XRD pattern of NiS/Cu_2S@N/S-C after discharge; (b) Partial enlargement curve in (a).

The anode materials were scraped from the collector (copper foil) for the *ex-situ* XRD test after discharge.

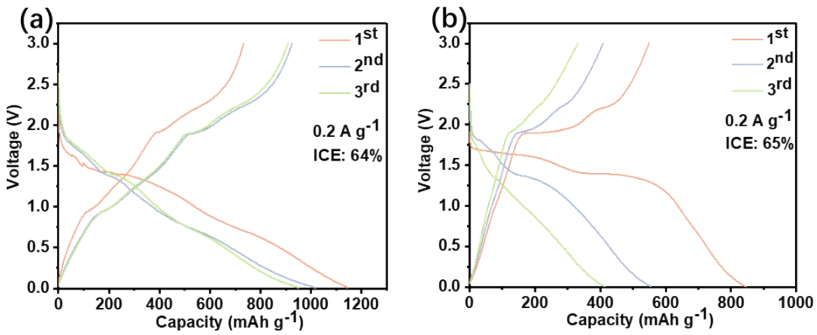

Fig. S7 Charge-discharge profiles of NiS@C and Pure-NiS at 0.2 A g^{-1}.

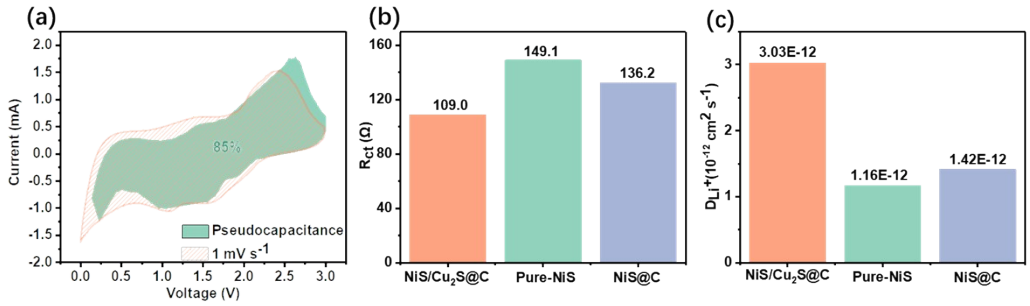

Fig. S8 (a) contribution rate of pseudo-capacitance of NiS/Cu_2S@N/S-C at 1 mV s^{-1}, (b)-(c) the values of R_{ct} and D_{Li}^{+} of NiS/Cu_2S@N/S-C, NiS@C and Pure-NiS.

The calculation of the lithium-ion diffusion coefficients

$$Z_{re} = \sigma_w \omega^{-0.5} + R_s + R_{ct} \quad \text{(S1)}$$

$$D_{Li^+} = 0.5\left(\frac{RT}{A_{ac}F^2\sigma_w C_{Li}}\right)^2 \quad \text{(S2)}$$

Where Z_{re}, ω, R, T, and C_{Li} are the real impedance in the low-frequency region, the angular frequency obtained from the low-frequency regime, the gas constant, the absolute temperature and the initial Li^+ molar concentration in the electrolyte (1 mol L^{-1}), respectively.

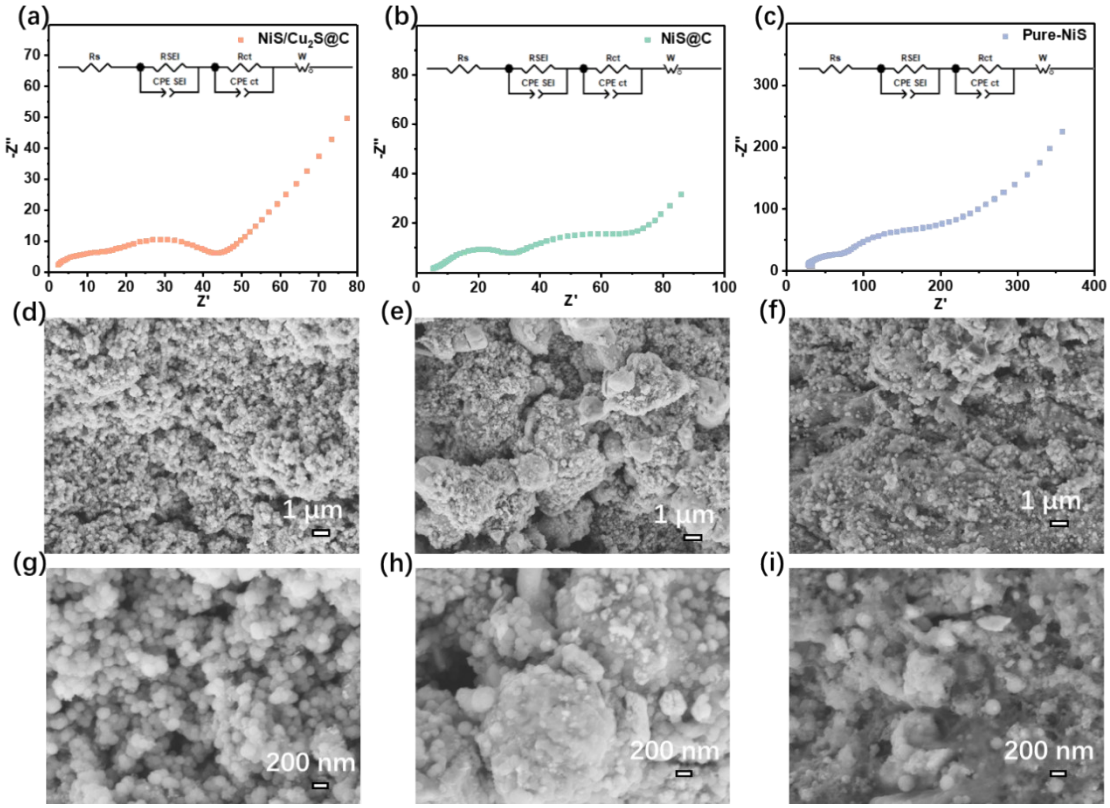

Fig. S9 (a)-(c) Nyquist plots of NiS/Cu_2S@S/N-C, NiS@C and Pure-NiS, SEM images of NiS/Cu_2S@ S/N-C, NiS@C and Pure-NiS at 1 A g^{-1} after 100 cycles at (d)-(f) low magnification and (g)-(i) high magnification, respectively.

Table S2. The resistance results of the NiS/Cu_2S@N/S-C, NiS@C and Pure-NiS after 100th cycles at 1 A g^{-1}

	NiS/Cu_2S@N/S-C	NiS@C	Pure-NiS
R_{SEI} (Ω)	43.7	85.5	294.5
R_{ct} (Ω)	23.1	34.4	86.0

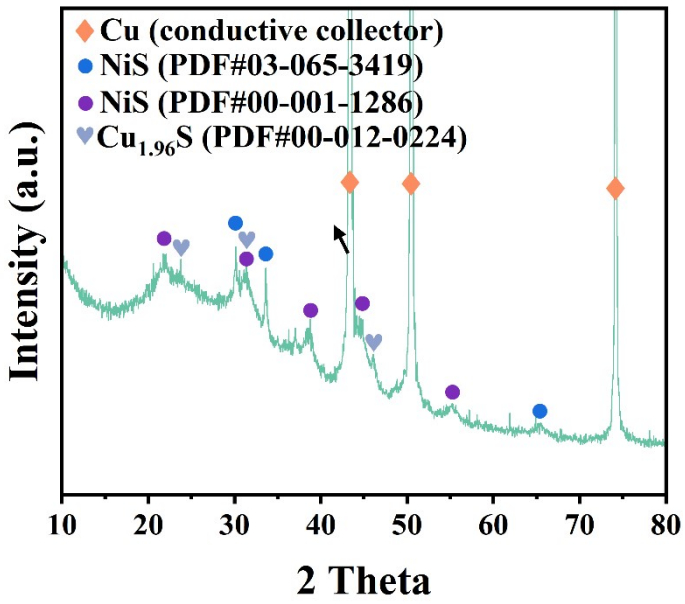

Fig. S10 The *ex-situ* XRD pattern of the NiS/Cu_2S@N/S-C after 350 cycles at 1 A g^{-1}

The characteristic peaks of NiS and $Cu_{1.96}S$ can still be clearly observed, which is consistent with the lithium storage mechanism mentioned in manuscript.

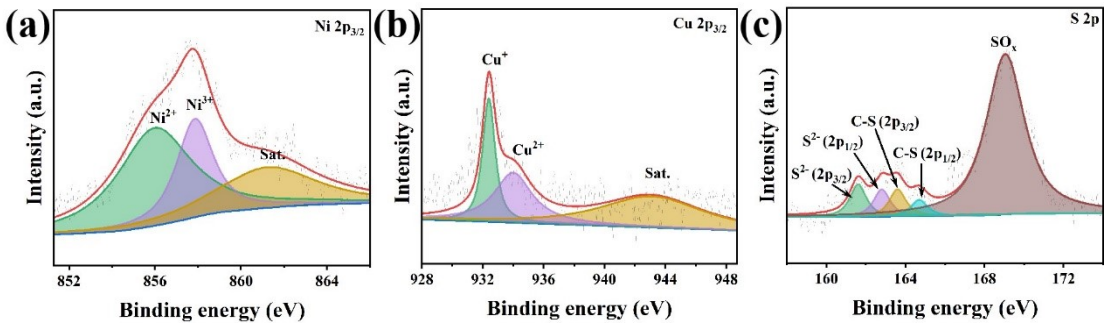

Fig. S11 The high-resolution XPS spectra in the regions of Ni 2p (a), Cu 2p (b), S 2p (c) for the NiS/Cu_2S@N/S-C after 350 cycles at 1 A g^{-1}

The existence of Ni^{2+} and Ni^{3+} can also be confirmed according to the spectrum of Ni $2p_{3/2}$ (Fig. S11a), which is similar to the pristine NiS/Cu_2S@N/S-C, suggesting the retention of NiS[3]. The high-resolution spectrum of Cu $2p_{3/2}$ (Fig. S11b) shows two obvious peaks at 932.4 and 934.0 eV, corresponding to the Cu^+ and Cu^{2+}, respectively[4], which is also similar to the pristine NiS/Cu_2S@N/S-C. As illustrated in Fig. S11c, the peaks of S $2p_{3/2}$ and $2p_{1/2}$ of S^{2-} (161.6 and 162.8 eV) further demonstrate the existence of NiS after long-term cyclings. The other two peaks at 163.8 and 165.1 eV can be attributed to the C-S bonding, demonstrating the retention of S-doped carbon matrix. In addition, the peak at 168.8 eV corresponds to the SO_x, which may be ascribed to the further surface oxidation in the air after the electrode taken apart from the tested coin cell[5].

References:

1. M. Lenoir, A. Grandjean, S. Poissonnet and D. R. Neuville, Quantitation of sulfate solubility in borosilicate glasses using Raman spectroscopy, *Journal of Non-Crystalline Solids*, 2009, **355**, 1468-1473.
2. A.R. Brough, A. Atkinson, Micro-Raman spectroscopy of thaumasite, *Cement and Concrete Research*, 2001, **31**, 421-424.
3. B. Guan, Y. Li, B. Yin, K. Liu, D. Wang, H. Zhang and C. Cheng, Synthesis of hierarchical NiS microflowers for high performance asymmetric supercapacitor, *Chemical Engineering Journal*, 2017, **308**, 1165-1173.
4. F. Han, W.-C. Li, D. Li and A.-H. Lu, In Situ Electrochemical Generation of Mesostructured Cu2S/C Composite for Enhanced Lithium Storage: Mechanism and Material Properties, *ChemElectroChem*, 2014, **1**, 733-740.
5. H. Qing, R. Wang, Z. Chen, M. Li, L. Zhang, Y. N. Zhou and R. Wu, In-situ embedding cobalt-doped copper sulfide within ultrathin carbon nanosheets for superior lithium storage performance, *J Colloid Interface Sci*, 2020, **566**, 1-10.